10. Engelking, P. C. *Rev. Sci. Instrum.* **1986**, *57*, 2274.
11. Suh, M. H.; Lee, S. K.; Rehfuss, B. D.; Miller, T. A.; Bondybey, V. E. *J. Phys. Chem.* **1991**, *95*, 2727.
12. Lee, S. K. *Bull. Korean Chem. Soc.* **1998**, *19*, 150.
13. Choi, I. S.; Lee, S. K. *Bull. Korean Chem. Soc.* **1995**, *16*, 281.
14. Lee, S. K. *Bull. Korean Chem. Soc.* **1995**, *9*, 795.
15. Choi, I. S.; Lee, S. K. *Bull. Korean Chem. Soc.* **1995**, *16*, 1089.
16. Choi, I. S.; Lee, S. K. *Bull. Korean Chem. Soc.* **1996**, *17*, 749.
17. Selco, J. I.; Carrick, P. G. *J. Mol. Spectrosc.* **1989**, *137*, 13.
18. Selco, J. I.; Carrick, P. G. *J. Mol. Spectrosc.* **1995**, *173*, 277.
19. Lee, S. K. *Bull. Korean Chem. Soc.* **1998**, *19*, 145.
20. Han, M. S.; Choi, I. S.; Lee, S. K. *Bull. Korean Chem. Soc.* **1996**, *17*, 991.
21. Wiese, M. L.; Smith, M. W.; Glennon, B. M. *Atomic Transition Probabilities*; NSRD-NBS4, 1986.
22. Pearse, R. W. B.; Gaydon, A. G. *The identification of Molecular Spectra*; 4th ed.; Chapman and Hall, London, U. K. 1976.
23. Lee, S. K.; Miller, T. A. *The 52nd International Symposium on Molecular Spectroscopy*; Columbus, Ohio, RI 09, June 16-20, 1997.
24. Kahane-Paillous, J.; Leach, S. *J. Chem. Phys.* **1958**, *55*, 439.
25. Hollas, J. M. *High Resolution Spectroscopy*, Butterworths: London, U.K., 1982.
26. Lee, S. K.; Suh, M. H.; Miller, T. A. *The 52nd International Symposium on Molecular Spectroscopy*; Columbus: Ohio, RI08, June 16-20, 1997.
27. Spangler, L. H.; Pratt, D. W. *Internal Rotation Dynamics from Electronic Spectroscopy in Supersonic Jets and Beams*; Hollas, J. M.; Phillips, D., Eds.; Blackie Academic & Professional: London, 1994.
28. Okuyama, K.; Mikami, N.; Ito, M. *J. Phys. Chem.* **1985**, *89*, 5617.
29. Takazawa, K.; Fujii, M.; Ito, M. *J. Chem. Phys.* **1993**, *99*, 3205.

A Study on the Sulfur-Resistant Catalysts for Water Gas Shift Reaction I. TPR Studies of Mo/γ-Al_2O_3 Catalysts

Jin-Nam Park, Joon-Hee Kim, and Ho-In Lee*

School of Chemical Engineering, Seoul National University, Seoul 151-742, Korea
Received August 27, 1998

Mo/γ-Al_2O_3 catalysts were prepared by impregnation method in various conditions to identify the states of surface Mo species. TPR (Temperature-Programmed Reduction) and Raman spectroscopy were applied to analyze the surface Mo species. TPR analysis revealed that MoO_3 was reduced to Mo through MoO_2, the intermediate state and the increase of Mo loading enhanced the reducibility of Mo oxide till the formation of monolayer coverage. High temperature calcination induced oxygen defects in MoO_3 giving their unstable states for easier reduction. Raman spectroscopy analysis showed that the increase of Mo loading induced the polymeric Mo oxide.

Introduction

Metal oxides which are supported on stable supports such as γ-Al_2O_3 and SiO_2 are widely used as catalysts for various chemical reactions. Supported metal oxides show different reduction behavior from unsupported ones. The difference of reduction property plays an important role in catalysis. The reduction of supported metal oxides could be hindered or promoted depending on the interaction between metal oxide and support. Nowak and Koros[1] reported that supported NiO has higher oxidation state than unsupported one. Holm and Clark[2] reported the formation of metal aluminate or metal silicate in supported metal oxide systems. The shape of supported metal oxides could be fine metal oxide form or metal oxide island form distributed homogeneously. In case of metal oxide island form, the reduction behavior is similar to that of unsupported metal oxide, and the support acts as dispersing agent and promotes the reduction of the oxide. In this condition, the rate equation of reduction is same as in unsupported metal oxide.

Metal atom or fine crystallite is mobile on the support.[3] The reduction of homogeneously supported metal oxide is proceeded by restructuring fine crystallites after the reduction of each metal ion or cluster resulting in the formation of large metal crystallites. This fine metal crystallite could promote the reduction by autocatalytic reaction. In case of Pt/γ-Al_2O_3, hydrogen spillover happens above 600 K.[4] If activated hydrogen atoms produced by autocatalytic reaction lose their mobility, the effect of autocatalytic reaction could be lost. There is possibility of inhibition to nuclei growth by the loss of metal mobility due to the strong interaction between metal and support.

*To whom all correspondence should be addressed.

TPR (Temperature-programmed reduction) is a widely used analytical technique to investigate the reduction behavior of metal oxides. The reaction order to hydrogen, activation energy for reduction, and rate constant for reduction could be obtained by the analysis of TPR curves with different temperature programming.[5-7] The reduction behavior of alumina-supported MoO_3 that is used as catalyst for hydrodesulfurization and water-gas shift reaction has been studied. Generally, alumina-supported MoO_3 shows two peaks in its TPR spectrum. One is low temperature peak (500-700 °C), and the other is high temperature peak (900-1100 °C), where the peak temperatures depend on the experimental condition. There are many interpretations on those peaks, but they are generally categorized into 3 cases of layer model,[8,9] bulk oxide reduction model,[10,11] and capping oxygen model.[12] The interpretation of TPR peak on alumina-supported MoO_3 was changed from layer model to bulk oxide reduction model, and lately capping oxygen model is suggested. There is no general agreement on the reduction behavior of supported MoO_3. The characterization of catalysts by TPR is easy and time saving, but the analysis of TPR profile is not easy. Therefore, the TPR technique could be an useful analytical method when assisted by other analytical instruments.

In the present study, we performed mainly TPR experiments for various alumina-supported molybdenum oxide samples. The TPR results were compared with the results of many previous studies proposing some advanced interpretations. We report here reduction properties and crystal structure types of the alumina-supported molybdenum oxide.

Experimental

Preparation of Catalysts. A series of xMA samples were prepared by impregnation of γ-Al_2O_3 (Catalysis Society of Japan, JRC-ALO-2) with an aqueous solution of $(NH_4)_6Mo_7O_{24}\cdot 4H_2O$ (Oriental, EP). The value x indicates the loading of the sample in wt% of MoO_3 to γ-Al_2O_3. Water was removed by a rotary vacuum evaporator at 50 °C. Thereafter the samples were dried at 105 °C in air for 2 hours, and finally calcined at 500 °C for 5 hours.

TPR/TPO Analysis. TPR apparatus shown in Figure 1 was used to investigate the surface structure and oxidation state of the samples. For these studies, a 40 mg of sample was placed on the sintered quartz frit inside a 10-mm-i.d. tube of fused quartz. For the reduction of the sample, an H_2 (1.5 sccm)/N_2 (28.5 sccm) flow gas was used and the heating rate was 10 °C/min. Peak temperature and area were determined by a curve fitting program using Gaussian type distribution.

Raman Analysis. Laser Raman spectra of the samples were obtained at room temperature using a spectrophotometer involving an Ar^+ ion laser (Spectra Physics, Model 2016) and double monochromator (Spex Ramalog, Model 1403). The samples were pressed into the form of pellets at a pressure of about 50 MPa for 2 minutes because the supported sample showed very low signal intensity. The smooth data of Raman analysis were acquired through a peak fitting program (Peakfit program).

BET Surface Area Analysis. Nitrogen (99.99%) and helium (99.99%) were used as adsorbate and inert gas, respectively in a commercial BET apparatus (Quantasorb M).

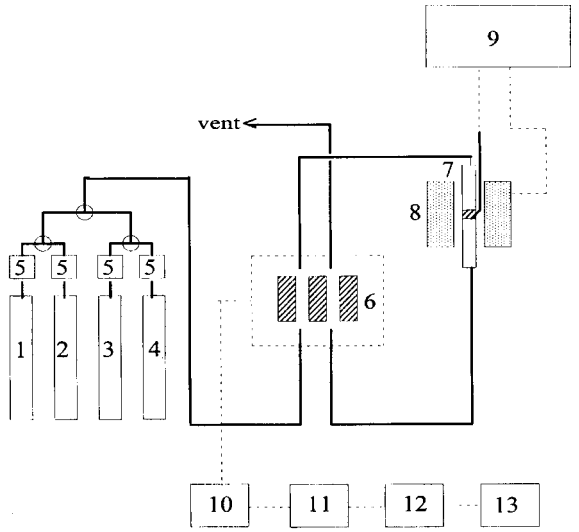

Figure 1. Schematic diagram of experimental apparatus used in TPR/TPO.

Results and Discussion

A series of samples with different Mo loadings were prepared for TPR study. Their BET surface areas are shown in Table 1. The surface area is decreased with the increase of Mo loading suggesting that Mo oxide particles plug pore mouths of the support. Theoretically, 10 wt% loading is enough to cover fully the support with a monolayer of Mo oxide.[13]

Figure 2 shows the TPR spectra of the samples with different Mo loadings. Two peaks are observed in the region of 500-670 °C (low temperature peak) and above 900 °C (high temperature peak), respectively. Generally, the higher concentration of hydrogen, the easier reduction of metal oxide. Shimada *et al.*[10] reported that the low temperature peak appeared at about 350 °C in a flow of 100% hydrogen for the 10 wt% MoO_3 sample calcined at 500 °C for 3 hours. Kadkhodayan and Brenner[11] reported that the low temperature peak appeared at about 540 °C in a flow of 5% hydrogen for the 2 wt% Mo sample calcined at 600 °C for 1 hour. Though the peak temperature is different, they showed same tendency of two-step reduction. Figure 2 reveals that the reduction of Mo oxide is easier with the increase of Mo loading. A peak is shown at about 700 °C with a different peak shape for the pure alumina support suggesting the removal of surface hydroxyl group by hydrogen. Successive TPR, TPO, and TPR results (Figure 3) show no reduction peak in the second TPR profile supporting our above

Table 1. BET surface areas of various xMA catalysts

Catalyst	BET S.A.(m^2/g)
0MA	193.4
2MA	189.6
5MA	189.1
10MA	162.3
30MA	136.3

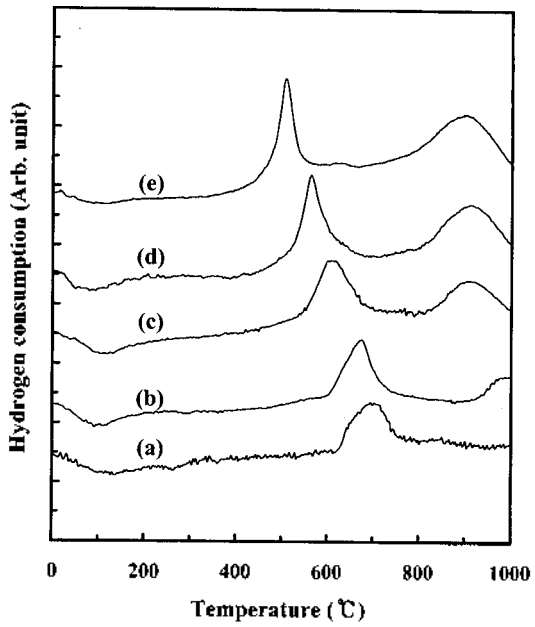

Figure 2. TPR profiles of (a) 0MA (alumina), (b) 2MA, (c) 5MA, (d) 10MA, and (e) 30MA.

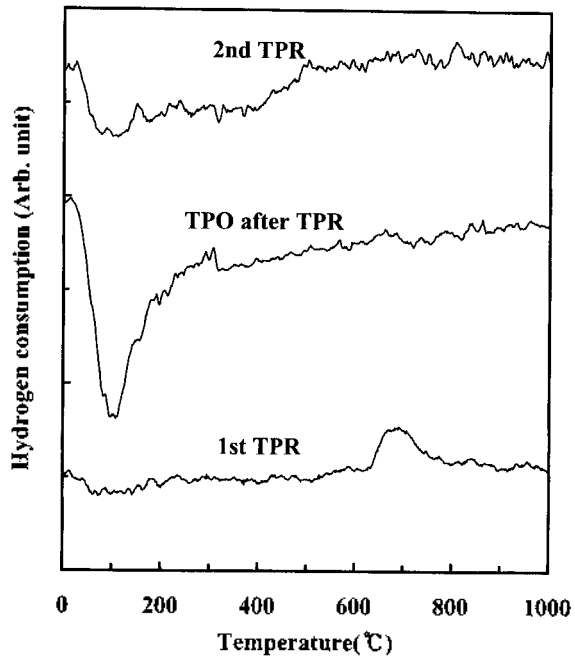

Figure 3. TPR profile of 0MA (alumina) and its successive TPR profile after TPO.

suggestion. Generally, there are two possibilities of reduction behavior when metal oxide is supported on a support. One is hindered reduction, and the other is promoted one. The former is caused by strong interaction between metal oxide and the support. In this case, the reduction is easier with the increase of metal loading because the interaction between metal oxide and the support becomes weaker. The latter is caused by fine dispersion of metal oxide with a little interaction between metal oxide and the support. In this case, the reduction is easier with the decrease of metal oxide loading because metal oxide particle size becomes smaller. However, in Figure 2, both the two peaks are shifted to lower temperatures with the increase of the loading before monolayer coverage (about 30 wt% in this study) suggesting that there is another factor to affect reduction behavior. We suppose a certain repulsive lateral interaction which is enhanced with the increase of the oxide loading till monolayer coverage resulting in easier reduction if we assume the same particle size in this region of coverage. Figure 2 suggests that the promoted reduction is applied to our system, and that the monolayer coverage is given by about 30 wt% MoO_3.

Figure 4 shows the TPR profiles of unsupported MoO_2 (Aldrich, 99%) and unsupported MoO_3 (prepared by the calcination of $(NH_4)_6Mo_7O_{24}\cdot 4H_2O$). MoO_2 shows no noticeable peak, but there is a slight increase in intensity for a reduction peak over 800 °C. Whereas MoO_3 shows a large reduction peak at about 800 °C increasing the intensity over 850 °C for the second reduction peak. From this result, it could be considered that the reduction temperature of MoO_3 to MoO_2 is about 800 °C in an unsupported system under this experimental condition.

Figure 5 shows the TPR profiles of three different samples with same amount of Mo metal loading, which are (a) physical mixture of MoO_2 and alumina, (b) physical mixture of MoO_3 and alumina, and (c) 10MA. Curve (a) shows no low temperature reduction peak at about 700 °C

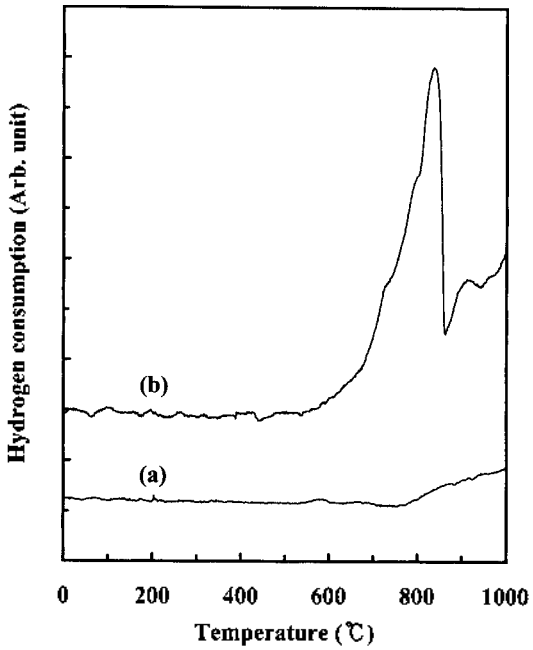

Figure 4. TPR profiles of (a) MoO_2 and (b) MoO_3.

and obvious high temperature one at about 950 °C. Both curves of (b) and (c) show clearly two characteristic reduction peaks. And physically mixed MoO_3 (curve b) shows low temperature peak at about 700 °C which is higher by 140 °C than in supported MoO_3 (curve c) and lower by 120 °C than in unsupported MoO_3 (Figure 4b). A small broad peak appeared in the range of 500-700 °C in curves (a) and (b) is suggested to be derived from the removal of surface hydroxyl group of the alumina which has no experience of calcination. This peak corresponds with that of 680 °C in the bottom curve of Figure 3. The shift of peak temperature to lower side in the mixed systems

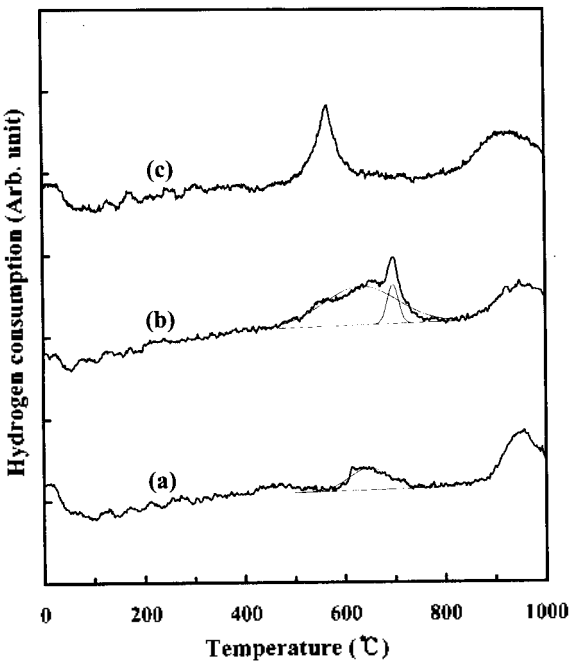

Figure 5. TPR profiles of (a) 10 wt% MoO_3 + alumina, (b) 10 wt% MoO_3 + alumina, and (c) 10MA (All samples contain the same amount of Mo metal.).

suggests that the promoted reduction mentioned above is shown even in the mixed system as well as in the supported system giving the medium promotion effect in the mixed system, and that the promotion effect is applied to both metal oxide and the support. The peak related to surface hydroxyl group in the curve (b) of Figure 5 appears at a sighly lower temperature than that of curve (a) suggesting that bulkier MoO_3 is more effective than MoO_2 in promoted reduction due to the difference in lateral interaction. The bottom curve of Figure 3 gives a corresponding peak at the highest temperature of about 700 °C because of no lateral interaction due to no loading of Mo oxide. This confirms again that the promotion reduction effect is applied even to the support. From the result, we suppose that the low and high temperature peaks are related with the reductions of MoO_3 to MoO_2 and of MoO_2 to Mo metal, respectively. When MoO_3 is mixed with alumina physically, the reduction is easier than in unsupported MoO_3. And the supported MoO_3 is much easily reduced compared with unsupported MoO_3. This suggests that the reduction is promoted by supporting, and alumina plays a role as dispersing agent. The same tendency was reported by Spanos *et al.*[14] in a titania-supported Mo system. Thomas *et al.*[8] and Kadkhodayan and Brenner[11] also reported same results in an alumina-supported Mo system, but explained the results unreasonably and simply in terms of interaction which is weaker by the agglomeration of metal oxide with the increase of Mo loading.

Three 10MA samples with different calcination temperatures of 500, 650, and 800 °C were prepared. Figure 6 shows their TPR profiles, and their peak temperatures and areas are in Table 2. Both low and high temperature peaks are shifted to lower temperatures with the increase of calcination temperature suggesting the formation of unstable

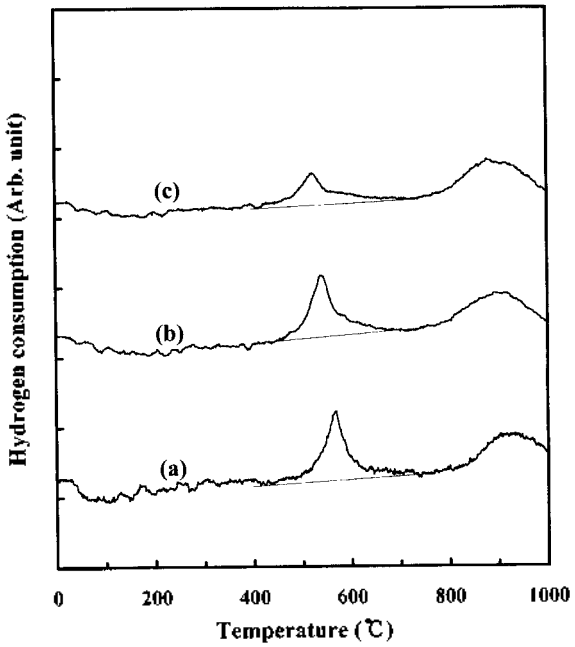

Figure 6. TPR profiles of 10MA calcined at (a) 500 °C, (b) 650 °C, and (c) 800 °C.

oxygen-defected state by the high temperature excitation. The area of low temperature peak is decreased with the increase of calcination temperature, while that of high temperature peak keeps almost constant, as shown in Table 2. This suggests that the amount of lattice oxygen for low temperature reduction would be decreased by high temperature calcination resulting in oxygen defects in the oxide lattice. This implies that a considerable amount of MoO_3 changed into MoO_2 or MoO_2-like state by high temperature calcination, and that the total amount of MoO_2 to be reduced to Mo should be same, *i.e.*, Table 2 says that more than 50% of MoO_3 is defected by the calcination at 800 °C. The areas of high temperature peak in Table 2 are different being due to the value from reduction upto 1000 °C in spite of an ideally same value. Calais *et al.*[15] and Wei *et al.*[16] reported similar results for unsupported Mo-sulfided and unsupported Mo-nitrided samples with different surface areas, respectively. The BET surface areas of the three samples are also shown in Table 2. The BET surface area is almost same suggesting that there is no change in structure of alumina and the oxygen defect of the metal oxide gives negligible effects to the BET surface area of the samples. The slight increase of BET surface area with the increase of calcination temperature is supposed to be due to oxygen vacancy. Arnoldy *et al.*[9] performed TPR experiment for 2.49 wt% Mo-

Table 2. TPR peak temperatures, TPR peak areas, and BET surface areas of various 10MA catalysts calcined at different temperatures

Calcination Temp.(°C)	1st peak temp.(°C)	1st peak area(a.u.)	2nd peak temp.(°C)	2nd peak area(a.u.)	BET S.A. (m^2/g)
500	566	33.0	927	30.2	162.3
650	540	32.1	900	33.2	165.3
800	524	16.4	892	33.6	169.1

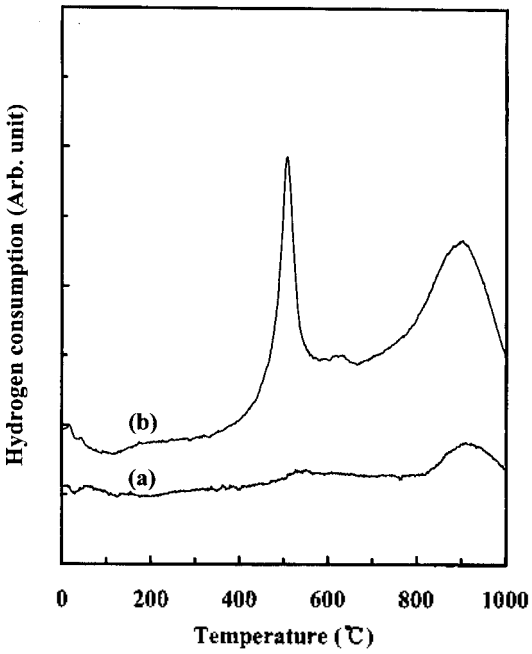

Figure 7. TPR profiles of (a) 30MA leached by 3% NH_4OH for 1 hour and (b) 30MA.

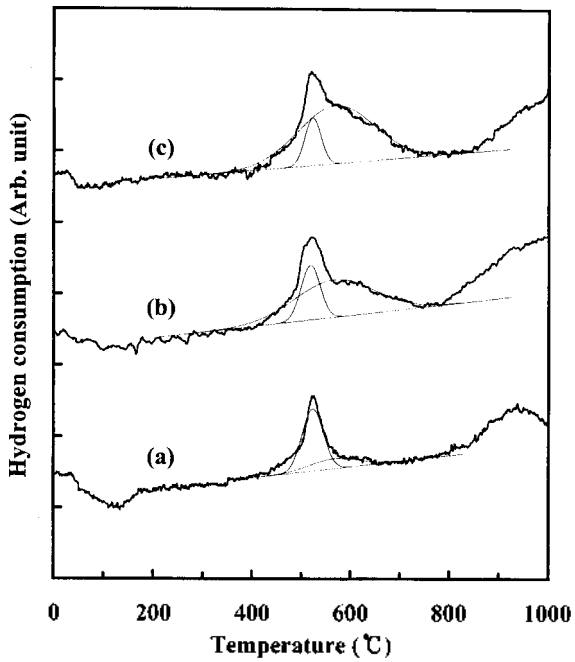

Figure 8. TPR profiles of (a) 30MA, (b) 50MA, and (c) 75MA.

loaded alumina samples with calcination temperature from 675 K to 1125 K. They used a conventional TPR system with a TCD cell as detector. They showed the reducibility of the samples was promoted by the increase of calcination temperature and Mo oxide on the surface started to sublime above 1100 K. Their results showed a same trend as those of Figure 6.

More TPR experiments were carried out with a 30MA sample treated by 3% aqueous ammonia following the experiments of Giordano *et al.*[17] They reported that polymeric octahedral molybdate was dissolved out by the treatment of aqueous ammonia remaining monomeric molybdate on the surface of the support. The treated sample shows no low temperature peak rejecting the capping oxygen model introduced in Introduction part. If the capping oxygen model is acceptable, low temperature peak would appear significantly regardless of the aqueous ammonia treatment because surface Mo still exists having oxygen even after the treatment. So, the appearance of low temperature reduction peak would be related with the existence of monomeric octahedral molybdate in multilayer state as reported by Giordano *et al.*[17] A tail peak appears in the low temperature reduction peak with the increase of Mo loading (Figures 2e and 7b). This implies the formation of another Mo oxide state in high metal loading over 10 wt% MoO_3. Such a tail peak also appears with the increase of calcination temperature (Figure 6) suggesting that this tail peak is related with the polymeric octahedral molybdate.

Figure 8 shows TPR profiles of 30MA, 50MA, and 75 MA samples with high MoO_3 loadings. Their peak temperatures and areas are shown in Table 3. In these samples with high MoO_3 loadings, the low temperature peak appears at almost same temperature. Curve fitting was carried out assuming the same peak temperatures for low temperature peak and tail peak, respectively, and the result of curve fitting was well matched with raw data. High temperature peak was impossible to apply curve fitting because the peak was still growing at the end of profile. High temperature peak shows a similar TPR profile to that of MoO_2 in Figure 4 when a large amount of MoO_3 is loaded. The tail peak of low temperature peak at about 560 °C is continuously grown with the increase of MoO_3 loading. When a small amount of Mo is loaded, the restricted amount of surface sites, which provide a direct interaction between Mo oxide and the support, are used first for the Mo oxide deposition on the surface. After these sites are consumed, another Mo oxide species, which interacts with the support weakly, is formed over the surface of the support without a certain value of saturation limit. This secondly formed Mo oxide species would have a similar structure to that of MoO_3 crystallite. However, the reduction of this species happens in lower temperature than in unsupported MoO_3 suggesting that there is still some interaction between Mo oxide and the support in this Mo oxide species. The existence of very small tail

Table 3. TPR peak temperatures and TPR peak areas of 30MA, 50MA, and 75MA catalysts

Catalyst	1st. peak temp. (°C)	1st. peak area (a.u.)	Tail peak temp. (°C)	Tail peak area (a.u.)	2nd. peak temp. (°C)	2nd. peak area (a.u.)
30MA	521	24.2	566	9.6	931	35.3
50MA	519	19.2	567	51.2	-	-
75MA	520	12.1	566	76.8	-	-

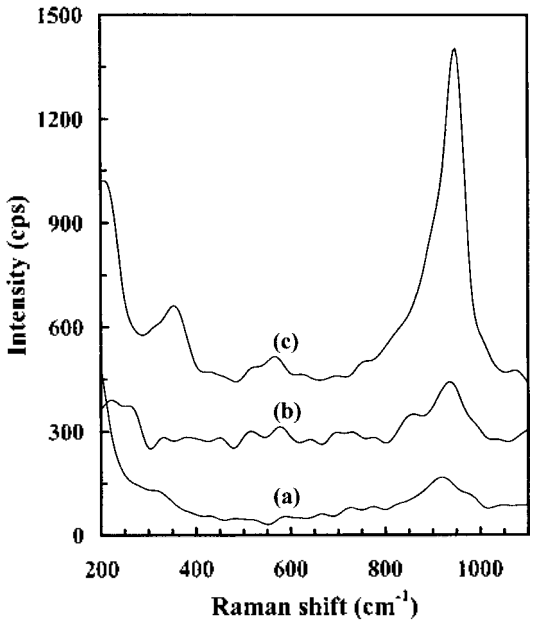

Figure 9. Raman spectra of (a) 5MA, (b) 10MA, and (c) 30MA.

peak of curve (a) suggests that the loading of 30 wt% is slightly passed over a monolayer coverage.

XRD analysis of alumina-supported Mo oxide samples were performed, but there was no significant peak due to the small amount of MoO_3 loading. The sample 30MA showed weak characteristic XRD peaks of MoO_3. Raman spectroscopy is a useful tool for the characterization of supported metal catalysts because amorphous supports such as alumina and silica show no characteristic peaks for Raman spectroscopy. Stencel[18] summarized Raman peak positions of various Mo oxide-related compounds. Kim *et al.*[19] reported that the Raman peak of 938-941 cm^{-1} represents the symmetric stretching of the terminal Mo=O of octahedrally coordinated $Mo_7O_{24}^{6-}$ and the peak of 320 cm^{-1} the Mo-O bending of tetrahedrally coordinated MoO_4^{2-}. And Brown *et al.*[20] reported that the Raman peak of 310-370 cm^{-1} ascribes to the bending of the terminal Mo=O of polmeric species. Figure 9 shows Raman spectra of 5MA, 10MA, and 30MA. A large peak is shown above 900 cm^{-1}, which would be caused by the terminal Mo=O of $Mo_7O_{24}^{6-}$ shifting from 920 cm^{-1} to 950 cm^{-1} with the increase of the loading. The result confirms that the amount of polymeric $Mo_7O_{24}^{6-}$ with large size increases with the increase of MoO_3 loading, and is agreed well with the results of the TPR analysis. The peak of 320 cm^{-1} reported by Kim *et al.*[19] is not shown in Figure 9 suggesting that the 5 wt% loading is too large to form significantly the monomeric species suggests that the capability of H_2O adsorption during exposure in air increases with the increase of Mo loading.[21]

Conclusions

Alumina-supported MoO_3 is reduced following the two-step reduction process, and more easily reduced than unsupported MoO_3. Reduction behavior of supported monolayer Mo oxide is different from that of supported multilayer Mo oxide. Two kinds of Mo oxide species are present on the surface of the support: one is monomeric molybdate which is easily reduced, and the other is polymeric molybdate similar to MoO_3 crystallite, which has no saturation limit and is formed after saturation of monomeric molybdate species.

Acknowledgment. This paper was supported by NON-DIRECTED RESEARCH FUND, Korea Research Foundation. The authors would like to thank both KRF for financial support and Catalysis Society of Japan for supplying alumina as the support.

References

1. Nowak, E. J.; Koros, R. M. *J. Catal.* **1967**, *7*, 50.
2. Holm, V. C. F.; Clark, A. *J. Catal.* **1968**, *11*, 305.
3. Rusckenstein, E.; Pulvermacher, B. *J. Catal.* **1973**, *29*, 224.
4. Kramer, R.; Andre, M. *J. Catal.* **1979**, *58*, 287.
5. Gentry, S. J.; Hurst, N. W.; Jones, A. *J. C. S. Faraday I* **1979**, *75*, 1688.
6. Falconer, J. L.; Schwarz, J. A. *Catal. Rev.-Sci. Eng.* **1983**, *25*, 141.
7. Monti, D. A. M.; Baiker, A. *J. Catal.* **1983**, *83*, 323.
8. Thomas, R.; van Oers, E. M.; de Beer, V. H. J.; Medema, J.; Moulijn, J. A. *J. Catal.* **1982**, *76*, 241.
9. Arnoldy, P.; Franken, M. C.; Scheffer, B.; Moulijn, J. A. *J. Catal.* **1985**, *96*, 381.
10. Shimada, H.; Sato, T.; Yoshimura, Y.; Hiraishi, J.; Nishijima, A. *J. Catal.* **1988**, *110*, 275.
11. Kadkhodayan, A.; Brenner, B. *J. Catal.* **1989**, *117*, 311.
12. Xie, X.; Yin, H.; Dou, B.; Huo, J. *Appl. Catal.* **1991**, *77*, 187.
13. Goldwasser, J.; Scott, C.; Josefina, M.; Zurita, P. *Catal. Lett.* **1995**, *32*, 273.
14. Spanos, N.; Matralis, H. K.; Kordulis, Ch.; Lycourghiotis, A. *J. Catal.* **1992**, *136*, 432.
15. Calais, C.; Matsubayashi, N.; Geantet, C.; Yoshimura, Y.; Shimada, H.; Nishijima, A.; Lacroix, M.; Breysee, M. *J. Catal.* **1998**, *174*, 130.
16. Wei, Z.; Xin, Q.; Grange, P.; Delmon, B. *J. Catal.* **1997**, *168*, 176.
17. Giordano, N.; Bart, J. C. J.; Vaghi, A.; Castellan, A.; Martinotti, G. *J. Catal.* **1975**, *36*, 81.
18. Stencel, J. M. In *Raman Spectroscopy for Catalysis*; Davis, B., Ed.; van Nostrand Reinhold Publications: New York, U. S. A., 1989; p 31.
19. Kim, D. S.; Segawa, K.; Soeya, T.; Wachs, I. E. *J. Catal.* **1992**, *136*, 539.